CrystEngComm

Accepted Manuscript

ROYAL SOCIETY
OF CHEMISTRY

www.rsc.org/crystengcomm

CrystEngComm RSCPublishing

ARTICLE

Cite this: DOI: 10.1039/x0xx00000x

Received 00th January 2012, Accepted 00th January 2012

DOI: 10.1039/x0xx00000x

www.rsc.org/

Guest induced head-to-tail columnar assembly of 5,17-difunctionalized calix[4]arene

Ryo Sekiya, Yutaro Yamasaki, Wataru Tada, Hidemi Shio and Takeharu Haino*

Calix[4]arene possessing two catechol side arms **1** and organic molecules (*n*PrOH, AcOH, AcOEt, and CH_3CN) crystallized to afford cocrystals: **1**•(*n*PrOH)$_4$, **1**•(AcOH)$_4$, **1**•(AcOEt), and **1**•(CH_3CN)$_2$. In these cocrystals, calix[4]arene **1** is arranged one-dimensionally, forming head-to-tail columnar structures. The organic guests settle in the residual space between the columnar structures; they are captured by the catechol side arms through hydrogen bonding. In the cocrystal **1**•(H_2O)$_2$, a continuous zigzag array of **1** is formed instead of the columnar assembly, demonstrating that the organic guests induced the formation of the head-to-tail columnar structures in the crystal packing. Crystalline apohost $\mathbf{1}_{\text{apo}}$ was prepared by the desorption of the MeOH guests from cocrystal **1**•(MeOH)$_4$; this compound adsorbed the MeOH vapour, reconstructing the original crystal packing. When $\mathbf{1}_{\text{apo}}$ adsorbed the *i*PrOH vapour, a cocrystal with a crystal structure similar to that of **1**•(MeOH)$_4$ was formed, suggesting that $\mathbf{1}_{\text{apo}}$ has a crystal structure similar to that of **1**•(MeOH)$_4$.

Introduction

Calix[*n*]arenes are macrocyclic compounds composed of *n* phenolic residues connected with each other in a cyclic array via methylene linkers. Their conformation, solubility, and functionality, such as the molecular recognition properties that constitute the important function of calix[*n*]arenes, can be controlled by introducing adequate substituents at the upper and lower rims, making calix[*n*]arenes the most popular macrocyclic hosts in supramolecular chemistry.[1] Within the calix[*n*]arene family, a small class of calix[*n*]arenes (n = 4,5) has attracted considerable attention for their synthetic flexibility and as molecular hosts in both solutions and the solid state.[2–5] For example, *p-tert*-butylcalix[4]arene[3] and *p*-sulphonatocalix[4]arene,[5] —well-known derivatives of calix[4]arene—recognize various molecules to form host-guest complexes with host-guest ratios of 1:1 and 2:1, depending on the molecular structures of the guests. Our group has been developing upper rim functionalised calix[4,5]arenes that exhibit unique guest encapsulation within their hydrophobic cavities.[6] A homoditopic host possessing two double calix[5]arene units encapsulates the C_{60} moieties of dumbbell-shaped cross-linkers to form supramolecular polymers.[6l,6t] 5,17-Difunctionalised 25,26,27,28-tatrapropyloxycalix[4]arene **1** forms a M_2L_3 triple-stranded helicate through coordination-driven self-assembly; the resulting helicate encapsulates pyridinium cations to form stable host-guest complexes in solution.[6s]

We recently found that calix[4]arene **1** forms an unusual head-to-tail polymeric columnar structure in the following cocrystals: **1**•(MeOH)$_4$, **1**•(EtOH)$_4$, **1**•(*i*PrOH)$_4$, and **1**•(BDO)$_2$ (Fig. 1).[7] (*i*PrOH = 2-propanol, BDO = 1,4-butandiol) Although columnar assemblies composed of calix[4]arenes have been reported in the liquid crystalline state,[8] few examples of crystalline materials have been reported so far.[9] Calix[4]arenes often form dimeric capsules[2h,5k] or one-dimensional up-down bilayer arrangements in the solid state.[5c] The head-to-tail polymeric columnar assembly represents another structural motif for calix[4]arenes, making research valuable.

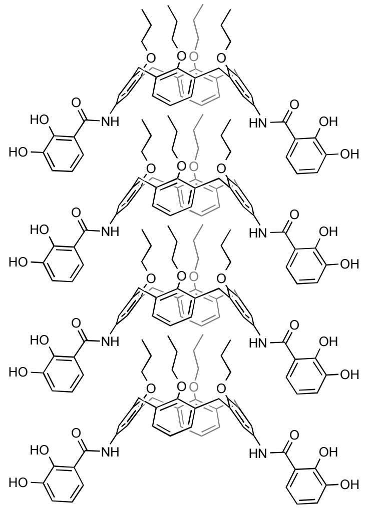

Fig. 1 Head-to-tail columnar structure of **1** found in the cocrystals.

Calix[4]arenes can include organic guests in their hydrophobic cavity, as observed in the *p-tert*-butylcalix[4]arene – toluene complex, and this complex is the first example of the crystal structure with the molecular arrangement in the solid state.[3a] In contrast, the organic guests are not included in the cavity in the four cocrystals; they settled in residual space between the columnar structures.[7] The difference in molecular recognition should be related to the formation of the columnar assembly, but additional X-ray crystal structures of the cocrystals are required. The cocrystals are characterised by their relatively high host-guest ratio. **1**•(BDO)$_2$

has a host-guest ratio of 1:2, while the other three have a host-guest ratio of 1:4,[7] suggesting that calix[4]arene **1** is an excellent host for small organic molecules. These results drove us to investigate the molecular recognition properties of **1** in the solid state, as well as how the functional groups of the guests affect the crystal packing, particularly in the head-to-tail columnar structure.

We herein report the X-ray crystal structures of the five cocrystals, **1**•(nPrOH)$_4$, **1**•(AcOH)$_4$, **1**•(AcOEt), **1**•(CH$_3$CN)$_2$, and **1**•(H$_2$O)$_2$ (nPrOH = 1-propanol). A head-to-tail columnar structure was formed in all cocrystals except for **1**•(H$_2$O)$_2$, demonstrating that the organic guests induced the crystal packing in a head-to-tail columnar manner. The excellent molecular recognition properties of **1** for small organic molecules is ascribed to the induced-fit adjustments of the relative location of the columnar structures for the organic guests and the presence of multiple hydrogen bond donor and acceptor sites on the catechol side arms. The absorption properties of crystalline apohost **1**$_{\text{apo}}$ prepared by desorbing the MeOH guests from **1**•(MeOH)$_4$ are also reported.

Experimental

Materials

All chemicals and solvents were purchased from Kanto Chemical Co., Ltd., Wako Pure Chemical Co., Ltd., Tokyo Kasei Kogyo Co., Ltd., and Sigma-Aldrich Co., Ltd., and were used as received without further purification. Calix[4]arene **1** was synthesised using a reported procedure.[6s]

Table 1 Crystallographic parameters

Crystal	**1**•(nPrOH)$_4$	**1**•(AcOH)$_4$	**1**•(AcOEt)	**1**•(CH$_3$CN)$_2$	**1**•(H$_2$O)$_2$
Guest	1-propanol	acetic acid	ethyl acetate	acetonitrile	water
Host-guest ratio	1 : 4	1 : 4	1 : 1	1 : 2	1 : 2
Formula	$C_{66}H_{90}N_2O_{14}$	$C_{62}H_{74}N_2O_{18}$	$C_{58}H_{66}N_2O_{12}$	$C_{58}H_{64}N_4O_{10}$	$C_{54}H_{62}N_2O_{12}$
Formula weight	1135.39	1135.23	983.12	977.13	931.05
Crystal system	Monoclinic	Monoclinic	Monoclinic	Triclinic	Monoclinic
Space group	$C2/c$ (#15)	$C2/c$ (#15)	$P2/c$ (#13)	$P\bar{1}$ (#2)	$P2/c$ (#13)
a / Å	35.683(11)	35.711(3)	15.402(2)	9.1552(9)	24.293(3)
b / Å	9.557(3)	9.0453(7)	18.320(2)	15.3084(15)	10.7595(13)
c / Å	17.733(6)	19.2477(15)	18.450(2)	18.302(2)	18.361(2)
α / °	90	90	90	96.349(1)	90
β / °	99.261(4)	109.063(1)	102.842(2)	94.785(1)	96.247(2)
γ / °	90	90	90	92.280(1)	90
V / Å^3	5969(3)	5876.4(8)	5076.0(10)	2537.4(4)	4770.6(10)
Z	4	4	4	2	4
d / g cm^{-3}	1.26	1.28	1.29	1.25	1.30
μ / mm^{-1}	0.088	0.094	0.090	0.085	0.091
Temperature / °C	–150	–150	–150	–150	–150
Crystal size / mm^3	0.21 × 0.15 × 0.005	0.21 × 0.12 × 0.08	0.05 × 0.03 × 0.02	0.09 × 0.06 × 0.04	0.28 × 0.14 × 0.03
Crystal form / colour	platelet / colourless	block / colourless	needle / colourless	platelet / colourless	platelet / colourless
2θ range / °	$4.4 \le 2\theta \le 44.7$	$4.3 \le 2\theta \le 58.0$	$3.5 \le 2\theta \le 52.7$	$4.5 \le 2\theta \le 50.5$	$4.1 \le 2\theta \le 50.5$
h range	$-38 \le h \le 32$	$-41 \le h \le 47$	$-19 \le h \le 19$	$-10 \le h \le 10$	$-29 \le h \le 29$
k range	$-10 \le k \le 7$	$-12 \le k \le 11$	$-22 \le k \le 21$	$-17 \le k \le 18$	$-12 \le k \le 11$
l range	$-18 \le l \le 18$	$-25 \le l \le 18$	$-10 \le l \le 23$	$-16 \le l \le 21$	$-15 \le l \le 22$
Total reflections	10028	17080	26473	11973	22349
Unique reflections	3836	7270	10321	8720	8607
R_{int}	0.0347	0.0180	0.0744	0.0195	0.0224
Observed reflections	3090	5748	5278	6338	6726
R_1 ^{a}	0.0403	0.0577	0.0744	0.0509	0.0627
wR_2 ^{b}	0.0937	0.1490	0.1411	0.1230	0.1656
G.O.F.	1.039	1.027	1.006	1.078	1.027
Parameters used	375	377	659	658	617
$\Delta\rho_{\text{max}}$ / eÅ^{-3}	0.471	0.591	0.387	0.386	0.567
$\Delta\rho_{\text{min}}$ / eÅ^{-3}	–0.268	–0.599	–0.245	–0.308	–0.531
CCDC	987474	987475	987476	987477	987478

^{a} $R_1 = (\Sigma||F_o| - |F_c||) / \Sigma|F_o|$. ^{b} $wR_2 = [\{\Sigma(w(F_o^2 - F_c^2)^2)\} / \Sigma(w(F_o^2)^2)]^{1/2}$.

Preparation of clathrate compounds

1•(nPrOH)$_4$, **1**•(AcOEt), and **1**•(CH$_3$CN)$_2$ were obtained by crystallizing **1** from nPrOH, AcOEt, and CH$_3$CN solutions, respectively. **1**•(AcOH)$_4$ were obtained by crystallizing **1** from an AcOEt solution containing AcOH. **1**•(H$_2$O)$_2$ were obtained from a 1-butanol solution.

The typical procedure used to prepare the cocrystals is as follows: approximately 1.7-2.0 mg (1.9–2.2 μmol) of **1** was dissolved in the solvent or the AcOEt solution containing AcOH. Colourless single crystals were obtained after the solutions standing for a few days at room temperature. The crystals were harvested and dried in air. **1**•(H$_2$O)$_2$ was stable in air, but the four cocrystals were not stable due to the desorption of the organic guests.

X-ray crystallography

The X-ray crystallographic data were collected on a Bruker SMART APEX-II ULTRA CCD diffractometer using graphite-monochromatized Mo Kα radiation (λ = 0.71073 Å) at –150 °C. The crystal structure was solved by the direct method with the SHELXS-2013 program and was refined by successive differential Fourier synthesis and full-matrix least-squares procedures with the SHELXL-2013 program.[10] The propyloxy chains in **1**•(AcOH)$_4$, **1**•(CH$_3$CN)$_2$, and **1**•(H$_2$O)$_2$ and one nPrOH guest in **1**•(nPrOH)$_4$ were disordered over two positions. Except for the disordered propyloxy chains in **1**•(H$_2$O)$_2$, anisotropic thermal factors were applied to all non-hydrogen atoms. EADP restraint was applied to the disordered atoms of **1**•(nPrOH)$_4$, **1**•(AcOH)$_4$, and **1**•(CH$_3$CN)$_2$. The hydrogen atoms on the nitrogen atoms and the carbon atoms, aside from those on the methyl groups, were generated geometrically. The positions of the hydrogen atoms on the methyl, hydroxyl, and carboxyl groups were estimated using the electron density maps. The hydrogen atoms on the water molecules in **1**•(H_2O)$_2$ were not generated. The crystallographic parameters, including the host-guest ratios of the clathrate compounds, are listed in Table 1. The intensities of the diffraction data for **1**•(*n*PrOH)$_4$ were weak because **1**•(*n*PrOH)$_4$ crystallized as thin platelet crystals, precluding the collection of a satisfactory number of the reflections. However, the parameters were well converged, and the crystal structure of **1**•(*n*PrOH)$_4$ is correct. The X-ray crystal structures were drawn using the Mercury program ver. 3.1. The guest accessible volume was calculated using the PLATON software package.[11]

The X-ray powder diffraction (XRD) data were collected on a Rigaku Rint-2000 X-ray diffractometer using graphite-monochromatized Cu Kα radiation (λ = 1.5418 Å) at room temperature with a scanning rate of 20 degree min^{-1}. XRD patterns were calculated with Mercury Program ver. 3.1.

Hirshfeld surface analysis

A Hirshfeld surface analysis was carried out using Crystal Explore ver. 3.0.[12] Parameters d_e and d_i are defined by the distances external and internal to the Hirshfeld surface, respectively, and parameter d_{norm} is a normalised contact distance defined by $d_{\text{norm}} = (d_i - r_i^{\text{vdW}}) / r_i^{\text{vdW}} + (d_e - r_e^{\text{vdW}}) / r_e^{\text{vdW}}$; r^{vdW} is the van der Waals radius of the appropriate atom internal or external to the surface. Detailed information regarding the Hirshfeld surface analysis, including parameters d_e, d_i, and d_{norm}, is described in the literature.

Preparation of apohost

A crystalline powder of apohost $\mathbf{1}_{\text{apo}}$ was prepared by desorbing the MeOH guests from **1**•(MeOH)$_4$ under reduced pressure at room temperature. The ^{1}H NMR spectrum of $\mathbf{1}_{\text{apo}}$ did not contain a signal corresponding to MeOH. Crystals of **1**•(MeOH)$_4$ were prepared using a previously reported method.[7] $\mathbf{1}_{\text{apo}}$ was stored in a desiccator under N_2.

Results and Discussions

Crystal structures

1•(*n*PrOH)$_4$ crystallized in the monoclinic crystal system with the space group *C*2/c (Fig. 2a).† The crystal packing is very similar to that of **1**•(EtOH)$_4$ and **1**•(*i*PrOH)$_4$.[7] Calixarene **1** has crystallographically-imposed twofold symmetry. The asymmetric unit contains half of **1** and two *n*PrOH guests. The ratio of **1** to *n*PrOH was 1:4. One of the two crystallographically independent *n*PrOH guests is disordered over two positions with a site occupancy factor (s.o.f.) of 0.550(3):0.450(3). The calix[4]arene adopts a pinched cone conformation; the two phenyl rings (rings B and D) squeeze inward, while the other rings possessing the catechol side arm (rings A and C) are tilted outward. Selected structural parameters are listed in Table 2. The propyloxy chains attached on the lower rim of the calix[4]arene adopt anti conformations. The catechol rings are twisted against rings A and C with a dihedral angle of 47.92(8)°.

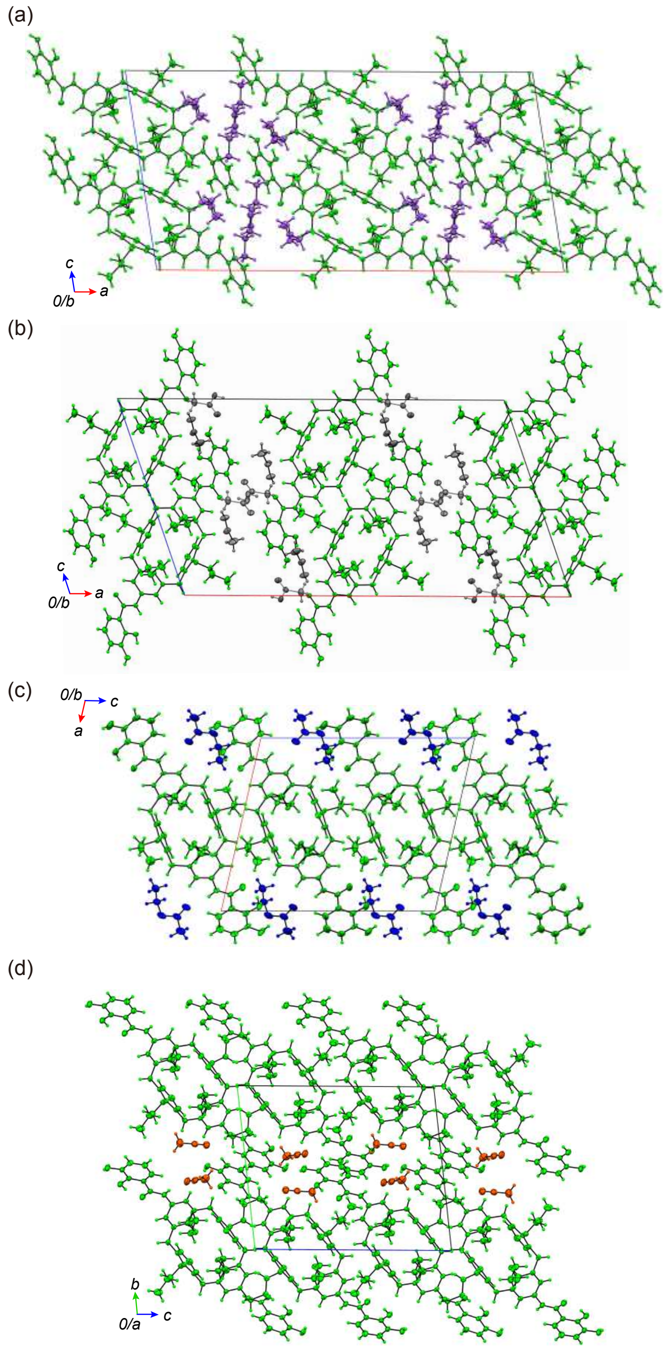

Fig. 2 ORTEP drawings of the X-ray crystal structures of (a) **1**•(*n*PrOH)$_4$, (b) **1**•(AcOH)$_4$, (c) **1**•(AcOEt), and (d) **1**•(CH_3CN)$_2$ viewed down along the *b* axis (a)-(c) and the *a* axis (d). (50% probability ellipsoids) Colour scheme: green (**1**), purple (*n*PrOH), grey (AcOH), blue (AcOEt), orange (CH_3CN). The disordered atoms with small s.o.f. are omitted for clarity.

Calix[4]arenes **1** are assembled in a head-to-tail manner along the [0 1 0] and [0 $\bar{1}$ 0] directions, forming polymeric columnar structures such that the terminal methyl groups of the propyloxy chains on rings A and C point to the cavity of the adjacent calix[4]arene (Fig. 3), whereas the propyloxy chains on rings B and D point outward. The nearest neighbours of the columnar structures are aligned in an antiparallel orientation to cancel out the local dipole moment. The period of the calix[4]arene array in the columnar structure is 9.6 Å. The *n*PrOH guests settled in the residual space formed between the columnar structures. Each hydroxyl group on the catechol rings captures one *n*PrOH guest via O–H···O hydrogen bonding (Fig. 4a). The oxygen atoms of the amide groups capture two *n*PrOH guests through bifurcated O–H···O hydrogen bonding.

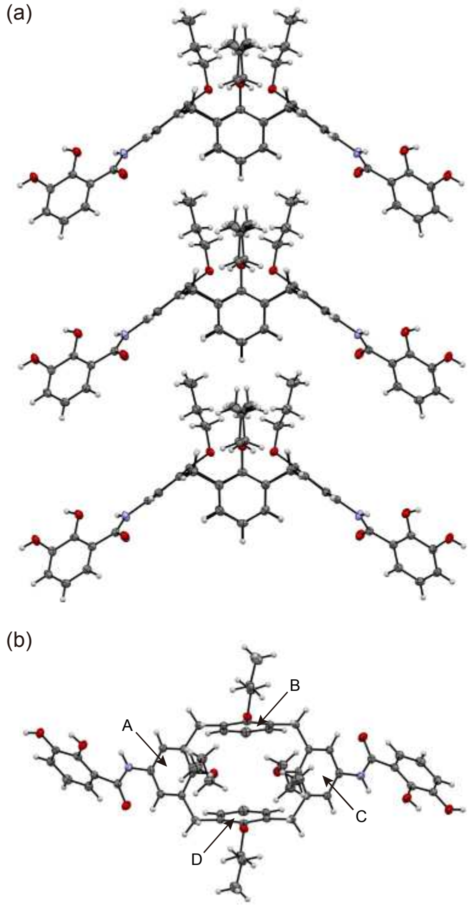

Fig. 3 ORTEP drawings of the (a) front and (b) top views of the head-to-tail columnar structure of **1** in **1**•(*n*PrOH)$_4$. Colour scheme: grey (carbon), white (hydrogen), light blue (nitrogen), red (oxygen). The head-to-tail columnar structures found in the other clathrate compounds are shown in ESI†.

1•(AcOH)$_4$ crystallized in the monoclinic crystal system with the space group *C*2/*c* (Fig. 2b).† Calixarene **1** has crystallographically-imposed twofold symmetry. The asymmetric unit contains half of **1** and two AcOH guests. The ratio of **1** to AcOH guests was 1:4. The molecular structure of **1** is almost the same as that of **1** in **1**•(*n*PrOH)$_4$. Selected structural parameters are listed in Table 2. The catechol rings are twisted against rings A and C with a dihedral angle of 32.64(8)°. The propyloxy chains on rings A and C are disordered over two positions with an s.o.f. of 0.846(3):0.154(3). The head-to-tail columnar structure is formed along the [0 1 0] and [0 $\bar{1}$ 0] directions. The columnar structure is very similar to that found in **1**•(*n*PrOH)$_4$. The period of the calix[4]arene array in the columnar structure is 9.1 Å, which is slightly shorter than that of **1**•(*n*PrOH)$_4$.

Carboxyl groups often form self-complementary pairwise O–H···O hydrogen bonds (graph set notation: $R_2^2(8)$)[13] to form a carboxylic acid dimer. Accordingly, carboxyl groups have been employed as a supramolecular synthon[14] in the field of the crystal engineering of purely organic[15] and organic-inorganic[16] hybrid crystals. However, no carboxylic acid dimers were formed between the AcOH guests. The carboxyl groups act as hydrogen bond acceptors and donors to form O–H···O hydrogen bonds with the hydroxyl groups on the catechol rings and the oxygen atoms of the amide groups (Fig. 4b). Calix[4]arene **1** has four hydroxyl groups and two amide groups and can form multiple hydrogen bonds. The observed hydrogen bonds may be energetically more favourable than the formation of the carboxylic acid dimer in **1**•(AcOH)$_4$.

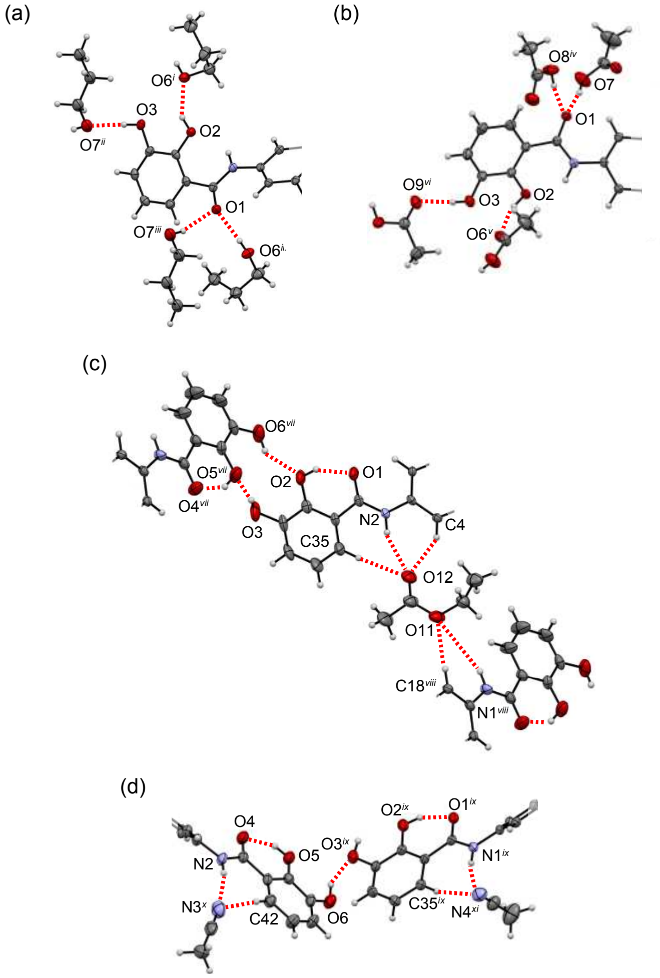

Fig. 4 Hydrogen bonds between **1** and the organic guest found in (a) **1**•(*n*PrOH)$_4$, (b) **1**•(AcOH)$_4$, (c) **1**•(AcOEt), and (d) **1**•(CH$_3$CN)$_2$. (50% probability ellipsoids) Colour scheme: grey (carbon), white (hydrogen), light-blue (nitrogen), red (oxygen). In (a), O1···O6^{i} = 2.807(1) Å; O1···O7^{ii} = 2.878(1) Å; O2···O6^{iii} = 2.651(1) Å; O3···O7^{iii} = 2.733(1) Å. In (b), O1···O7 = 2.661(1) Å; O1···O8^{iv} = 2.664(1) Å; O2···O6^{v} = 2.699(1) Å; O3···O9^{vi} = 2.689(1) Å. In (c), O2···O6^{vii} = 2.773(1) Å; O3···O5^{vii} = 2.878(1) Å; O12···C35 = 3.374(1) Å; O12···N2 = 3.133(1) Å; O12···C4 = 3.245(1) Å; O11···C18^{viii} = 3.511(1) Å; O11···N1^{viii} = 3.961(1) Å. In (d), N3^{x}···N2 = 3.397(1) Å; O6···O3^{ix} = 2.745(1) Å; N3···C42 = 3.398(1) Å; N4^{xi}···N1^{ix} = 3.145(1) Å; N1^{xi}···C35^{ix} = 3.633(1) Å. In (a), the disordered atoms with small s.o.f. are omitted for clarity. Symmetry codes: *i* = –*x*+1/2, –*y*+1/2, –*z*; *ii* = x, –y+1, Z–1/2; *iii* = –*x*+1/2, *y*+1/2, –*z*+1/2; *iv* = –*x*+1/2+1, *y*+1/2, –*z*+1/2; *v* = *x*, –*y*+1 *z*–1/2; *vi* = *x*, *y*+1, *z*–1; *vii* = *x*–1, *y*, *z*–1; *viii* = *x*–1, *y*, *z*; *ix* = *x*, *y*–1, *z*+1; *x* = *x*+1, *y*, *z*; *xi* = *x*+1, *y*, *z*+1

1•(AcOEt) crystallized in the monoclinic crystal system with the space group *P*2/*c* (Fig. 2c).† The asymmetric unit contains one molecule of **1** and one AcOEt guest. The ratio of **1** to the AcOEt guest was 1:1; this ratio is the smallest among the nine clathrate compounds. Selected structural parameters for **1** are listed in Table 2. In contrast to **1**•(*n*PrOH)$_4$ and **1**•(AcOH)$_4$, the catechol rings are almost coplanar to rings A and C with a dihedral angle of 3.4(2)° and 10.7(2)°, respectively. The hydroxyl groups and the oxygen atom of the amide group point in the same direction, while the hydroxyl group at the *o*-position of the catechol ring forms intramolecular hydrogen bonds with the oxygen atom of the amide group (graph set notation: S(6)).[13] The propyloxy chains on rings A and C adopt an anti conformation, while those on rings B and D adopt a gauche conformation. The head-to-tail columnar structure is formed in the [0 1 0] and [0 $\bar{1}$ 0] directions. The period of the calix[4]arene array in the columnar structure is 9.1 Å, remaining similar in length to that of **1**•(AcOH)$_4$.

Table 2. Selected structural parameters for **1**

Crystal	Angle /° (ring A and ring C) [a]	Angle /° (ring B and ring D) [a]	Distance /Å (ring A and ring C) [b]	Distance /Å (ring B and ring D) [b]
1•(*n*PrOH)$_4$	76.55(6)	24.24(9)	7.70	4.70
1•(AcOH)$_4$	69.95(4)	23.81(6)	7.76	4.71
1•(AcOEt)	71.02(7)	18.20(13)	7.71	4.85
1•(CH$_3$CN)$_2$	71.43(6)	18.25(12)	7.72	4.87
1•(H$_2$O)$_2$	3.4(2)	89.71(8)	5.21	7.51

[a] Inter-annular aromatic angle. [b] Inter-centroid distance.

Interestingly, exchanging the carboxyl group with the ethyl ester group resulted in a different host-guest interaction. The AcOEt guest is captured by N–H···O and two C–H···O hydrogen bonds (Fig. 4c). No hydrogen bonds were formed between the hydroxyl group and the AcOEt guest. Instead, the catechol ring forms $R_2^2(10)$ hydrogen bonds with the catechol ring of **1** in the neighbouring columnar structure.

1•(CH$_3$CN)$_2$ crystallized in the triclinic crystal system with the space group $P\bar{1}$ (Fig. 2d).† The asymmetric unit contains one molecule of **1** and two CH$_3$CN guests. The ratio of **1** to CH$_3$CN guests was 1:2. Selected structural parameters for **1** are listed in Table 2. The catechol rings are twisted against rings A and C with dihedral angles of 52.40(8)° and 37.02(10)°, respectively. The hydroxyl groups and the oxygen atom of the amide group point in the same direction, while a S(6) hydrogen bond is formed between the hydroxyl group on the *o*-position of the catechol ring and the oxygen atom of the amide group. The propyloxy chains adopt an anti conformation; those on ring D are disordered over the two positions with a s.o.f. of 0.703(4):0.297(4). The head-to-tail columnar structure forms along the [1 0 0] and [$\bar{1}$ 0 0] directions. The columnar structure is very similar to that found in the other clathrate compounds. The period of the calix[4]arene array in the columnar structure is 9.2 Å.

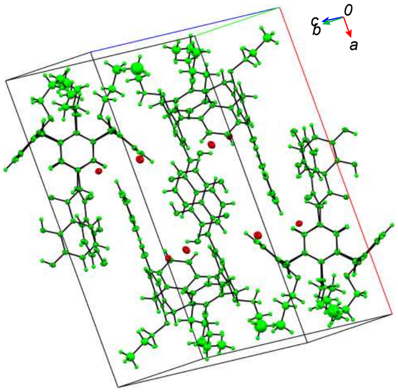

Fig. 5 ORTEP drawing of the X-ray crystal structure of **1**•(H$_2$O)$_2$. (50% probability ellipsoids) Colour scheme: green (**1**), red (H$_2$O). The propyloxy chains were refined isotropically. The disordered atoms with small s.o.f. are omitted for clarity.

The host-guest interaction between **1** and the CH$_3$CN guest is similar to that in **1**•(AcOEt); the CH$_3$CN guests are captured by N–H···O and C–H···O hydrogen bonds, while no hydrogen bonds are formed between the hydroxyl group and the CH$_3$CN guest. The hydrogen bond is formed between the hydroxyl groups at the *m*-position of the catechol rings.

To investigate the effect of the organic guests on the formation of the head-to-tail columnar structure, we attempted to prepare a crystal of **1** alone. Although, the target crystal could not be obtained, crystals of **1**•(H$_2$O)$_2$ were obtained from a 1-butanol solution.

The crystal structure of **1**•(H$_2$O)$_2$ demonstrates that having no included organic guests considerably changed the crystal packing (Fig. 5). **1**•(H$_2$O)$_2$ crystallized in the monoclinic crystal system with the space group of $P2/c$.† The asymmetric unit contains one molecule of **1** and two molecules of water. The ratio of **1** to the H$_2$O guests was 1:2. The structure of the calix[4]arene differs from those found in the clathrate compounds; rings A and C possessing the catechol side arms squeeze inward, while rings B and D are tilted outward (Fig. 6a and 6b). Selected structural parameters are listed in Table 2. The catechol ring is twisted against ring A (66.43(8)°) while the other is almost parallel to ring C (10.5(2)°). Consequently, an intramolecular C–H/π interaction (2.96 Å) forms between the catechol rings. No space is available for the inclusion of the propyloxy chains in the calix[4]arene, and a zigzag array of **1** is formed along the [0 1 1] directions instead of the head-to-tail columnar structure (Fig. 6c). The propyloxy chains adopted anti and gauche conformations and are disordered over two positions. The s.o.f. of the propyloxy chains on rings A, B, C, and D are 0.75(1):0.25(1), 0.55(1):0.45(1), 0.549(7):0.451(7), and 0.69(1):0.31(1), respectively. The water guests are captured by the hydroxyl group at the *m*-position of the catechol ring and the hydrogen atom of the amide group.

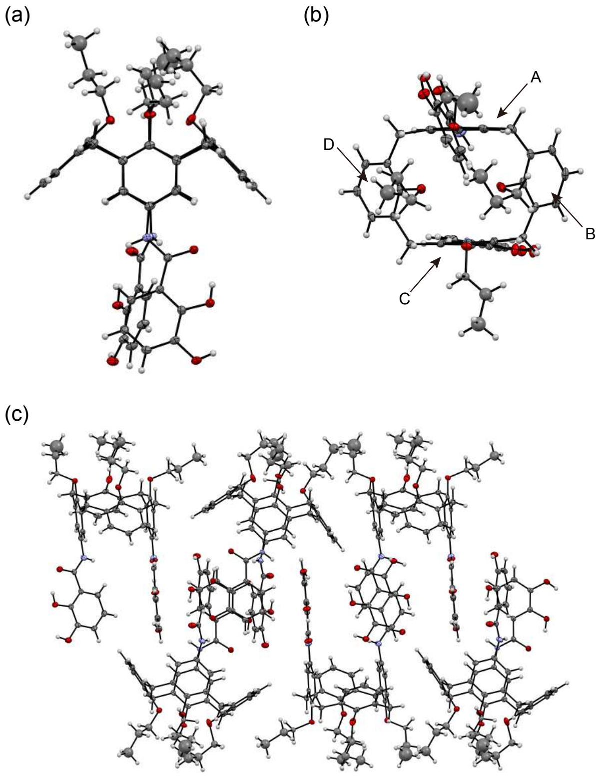

Fig. 6 ORTEP drawings of (a) the front and (b) top views of **1** and (c) the zigzag array of **1** found in **1**•(H$_2$O)$_2$. (30% probability ellipsoids) Colour scheme: grey (carbon), white (hydrogen), light-blue (nitrogen), red (oxygen). The propyloxy chains were refined isotropically. The disordered atoms with small s.o.f. are omitted for clarity.

Hirshfeld surface analysis

The Hirshfeld surface analysis of the four cocrystals, **1**•(*n*PrOH)$_4$, **1**•(AcOH)$_4$, **1**•(AcOEt), and **1**•(CH$_3$CN)$_2$, was carried out to investigate the intermolecular contacts between the propyloxy chains and the cavity of the calix[4]arene. Calix[4]arene **1** possessing the disordered propyloxy chains with higher s.o.f. was used for the Hirshfeld surface analysis of **1**•(AcOH)$_4$ and **1**•(CH$_3$CN)$_2$. Fig. 7a shows the top and bottom views of the 3D isosurface picture of the Hirshfeld surface mapped with d_{norm} of **1** in **1**•(*n*PrOH)$_4$. The terminal methyl groups of the propyloxy chains and the cavity of the calix[4]arene are coloured white-to-blue. The Hirshfeld surfaces of **1** in the other three cocrystals exhibited a similar colour distribution. Therefore, the intermolecular contacts are near van der Waals separations, and accordingly, the steric complementarity between the terminal methyl groups and the cavity of the calix[4]arene direct the continuous columnar array of **1**.

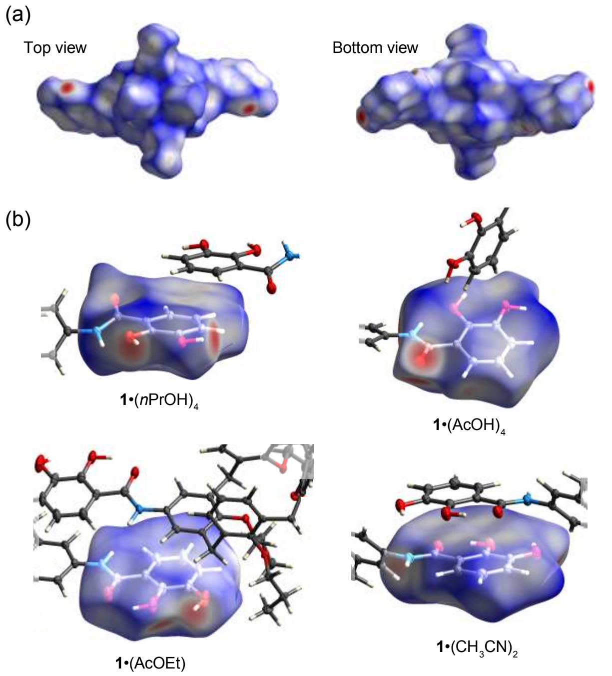

Fig. 7 Three-dimensional (3D) isosurface pictures of the Hirshfeld surfaces mapped with the d_{norm} of (a) **1** in **1**•(*n*PrOH)$_4$ and (b) the catechol rings of **1** in **1**•(*n*PrOH)$_4$ (top, left), (b) **1**•(AcOH)$_4$ (top, right), (c) **1**•(AcOEt) (bottom, left), and **1**•(CH$_3$CN)$_2$ (bottom, right). The 3D isosurface pictures of the d_{norm} parameter are coloured as follows: red for contacts shorter than van der Waals separations, white for contacts on van der Waals separations, and blue for contacts greater than van der Waals separations.

Fig. 7b displays the Hirshfeld surfaces of the catechol side arms in the four clathrate compounds, showing that the edge and surface of the catechol side arm interact with the organic guest and the host of the neighbouring columnar structure, respectively, and that the interactions between the hosts differ from each other. The regions coloured in red at the edge of the catechol side arms denote hydrogen bonding between calix[4]arene **1** and the organic guest. The surface of the catechol side arms interacts with the catechol side arm (**1**•(*n*PrOH)$_4$, **1**•(AcOH)$_4$, and **1**•(CH$_3$CN)$_4$) or the aromatic ring of the calix[4]arene (**1**•(AcOEt)) through a π-π stacking or C–H/π interaction. In **1**•(*n*PrOH)$_4$ and **1**•(AcOH)$_4$, the interactions are relatively strong, as demonstrated by the reddish region on the Hirshfeld surfaces. In **1**•(AcOEt) and **1**•(CH$_3$CN)$_2$, the distances between the two aromatic rings are near the van der Waals separation, and the π-π stacking interactions are weak compared to that in **1**•(*n*PrOH)$_4$.

Columnar structure and inclusion properties

The crystal structures of **1**•(*n*PrOH)$_4$, **1**•(AcOH)$_4$, **1**•(AcOEt), **1**•(CH$_3$CN)$_2$, and **1**•(H$_2$O)$_2$ and those of the previously reported four clathrate compounds demonstrate that the columnar structure is formed only when calix[4]arene **1** cocrystallized with the organic guests. Specifically, the organic guests induce the head-to-tail columnar organization in the crystal packing. The Hirshfeld surface analysis demonstrated that the terminal methyl groups resulted in only weak van der Waals interactions to the cavity of the calix[4]arene. However, the columnar assemblies were found in all clathrate compounds, except for **1**•(H$_2$O)$_2$, without apparent distortion in their structures by the hydrogen bonds between **1** and the organic guest. The strong tendency toward the head-to-tail columnar assembly is of interest because hydrogen bonding is a relatively strong intermolecular interaction that could change the crystal packing, including the columnar assembly. This tendency most likely occurs due to the molecular structure of **1**, which consists of hydrophilic catechol side arms and a hydrophobic calix[4]arene moiety. The organic guests interact selectively with the hydrogen bond donor and acceptor sites of the catechol side arms, as demonstrated by the X-ray crystal structures and the Hirshfeld surface analysis; the calix[4]arene moieties form columnar structures without interference by the coexisting organic guests. The columnar assembly can be regarded as a host-guest complex of the hydrophobic propyloxy chains and the hydrophobic cavity of the calix[4]arene.

Table 3 Host-guest (H–G) ratios, solvent accessible volumes (V_{guest}), volumes of the unit cell (V_{cell}), and $V_{\text{guest}}/V_{\text{cell}}$ (%) for the eight clathrate compounds.

Crystal	H–G ratio	V_{guest} ^{a} / Å^3	V_{cell} / Å^3	$V_{\text{guest}}/V_{\text{cell}}$ (%)
1•(MeOH)$_4$ ^{b}	1 : 4	1016	5397.4(5)	18.8
1•(EtOH)$_4$ ^{b}	1 : 4	1340	5707.5(11)	23.5
1•(*n*PrOH)$_4$	1 : 4	1624	5969(2)	27.2
1•(*i*PrOH)$_4$ ^{b}	1 : 4	1872	6177.8(5)	30.6
1•(BDO)$_2$ ^{b}	1 : 2	1176	5597(3)	21.0
1•(AcOH)$_4$	1 : 4	1446	5876.4(2)	24.6
1•(AcOEt)	1 : 1	644	5076.0(3)	12.7
1•(CH$_3$CN)$_2$	1 : 2	321	2537.25(6)	12.7

^{a} V_{guest} was calculated by the PLATON program.[11] ^{b} See ref. 7.

Table 3 lists the host-guest ratios, the solvent accessible volumes (V_{guest}), the volumes of the unit cell (V), and the $V_{\text{guest}}/V_{\text{cell}}$ (%) of the eight clathrate compounds. The host-guest ratio depends on the functional groups of the organic guests. The alcohol molecules and AcOH act as hydrogen bond donors and acceptors to form the cocrystals with host-guest ratios of 1:4, except for **1**•(BDO)$_2$. The high host-guest ratio is ascribed to the four hydroxyl groups in **1**, each of which captures one organic guest. For BDO, both sides of the hydroxyl groups of BDO participate in hydrogen bonding, resulting in the lower host-guest ratio.[7] In contrast, the host-guest ratios of AcOEt and CH$_3$CN are low because only two amide groups are present in **1**. However, the lack of participation by the hydroxyl groups remains uncertain. Similar hydrogen bonds should form because AcOEt and CH$_3$CN act only as hydrogen bond acceptors.

In contrast to the columnar structures that remain similar throughout the cocrystals, the relative location of the columnar structures is variable for the organic guests, indicating that $V_{\text{guest}}/V_{\text{cell}}$ changes from 12.7% to 30.6%, depending on the molecular structures of the guests. This adjustability altered the interactions between the hosts, as shown in Fig. 7b. The induced-fit adjustments and the presence of the hydrogen bond donor and acceptor sites on the catechol side arms are responsible for the excellent molecular recognition properties of **1** in the solid state.

Desorption and absorption of organic guests

Calix[4]arene **1** forms multiple hydrogen bonds, suggesting that the crystalline apohost should be able to adsorb vaporised organic guests. We prepared apohost $\mathbf{1}_{apo}$ from **1**•$(MeOH)_4$ because the MeOH guests are quickly desorbed from **1**•$(MeOH)_4$. Fig. 8a displays the XRD pattern of $\mathbf{1}_{apo}$, and Figs 8b and c display the calculated XRD patterns of **1**•$(MeOH)_4$ and **1**•$(H_2O)_2$, respectively. The desorption of the MeOH guests induced a crystal phase transition. The XRD pattern of $\mathbf{1}_{apo}$ is different from that of **1**•$(H_2O)_2$, suggesting that the zigzag array found in **1**•$(H_2O)_2$ was not formed. After exposing $\mathbf{1}_{apo}$ to MeOH vapour for 24 h at room temperature, the crystal structure returned to the original crystal packing (Fig. 8d, 0 min). The adsorbed MeOH guests were quickly desorbed from reconstructed **1**•$(MeOH)_4$ to afford $\mathbf{1}_{apo}$. The crystal phase transition was followed using XRD (Fig. 8d, 3, 6, and 9 min). No intermediate crystal phases were found in the XRD patterns, indicating that the crystal phase transition occurred between only two crystal phases. The crystal phase transition between **1**•$(MeOH)_4$ and $\mathbf{1}_{apo}$ could be repeated several times. Therefore, $\mathbf{1}_{apo}$ exhibits flexible crystal packing, and columnar structures similar to those found in **1**•$(MeOH)_4$ are preserved in $\mathbf{1}_{apo}$, enabling the absorption of MeOH vapour and the reconstruction of the original crystal packing.

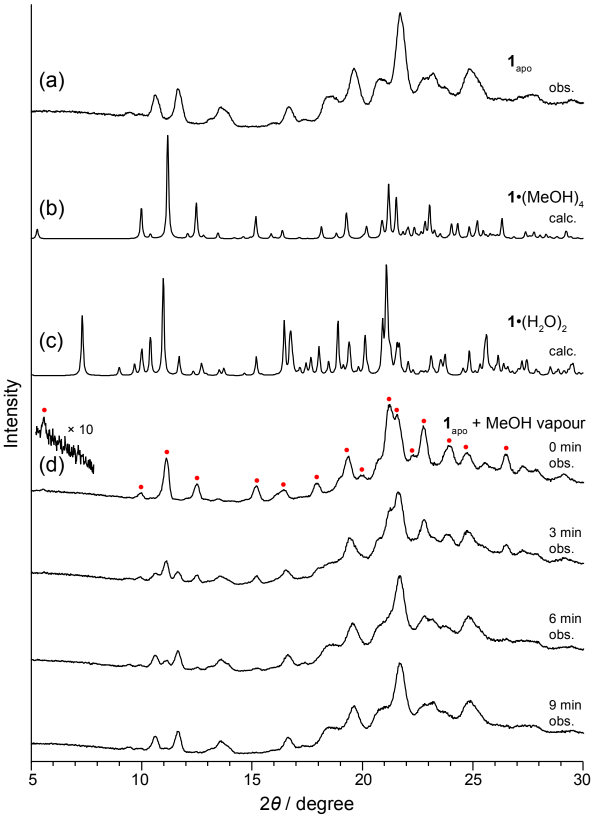

Fig. 8 Observed and calculated X-ray powder diffraction patterns (5° ≤ $2\theta \leq$ 30°) of (a) $\mathbf{1}_{apo}$, (b) **1**•$(MeOH)_4$, (c) **1**•$(H_2O)_2$, and (d) $\mathbf{1}_{apo}$+MeOH after standing for 0, 3, 6, and 9 min at room temperature. The red circles denote the diffractions of **1**•$(MeOH)_4$. Scan rate = 20 degree min^{-1}.

The orientation of the columnar structures formed in **1**•$(MeOH)_4$ differs from those formed in the other clathrate compounds, such as **1**•$(i\text{PrOH})_4$ (Fig. 9a). We investigated whether the orientation of the columnar structures formed in **1**•$(MeOH)_4$ is preserved in $\mathbf{1}_{apo}$ and whether this orientation is changed by the adsorption of *i*PrOH vapour. Fig. 9b displays the XRD patterns of $\mathbf{1}_{apo}$ after exposure to *i*PrOH vapour for 24 h at room temperature. The XRD pattern differs from that calculated for **1**•$(i\text{PrOH})_4$ (Fig. 9d) but remains similar to that of **1**•$(MeOH)_4$ (Fig. 9c). The *i*PrOH guests remained adsorbed in the powder for at least 10 min. The similar XRD pattern indicates that $\mathbf{1}_{apo}$ adsorbed the *i*PrOH vapour to form a cocrystal with a crystal structure similar to that of **1**•$(MeOH)_4$. Therefore, the orientation of the columnar structures formed in **1**•$(MeOH)_4$ was preserved in $\mathbf{1}_{apo}$, remaining unchanged after the adsorption of *i*PrOH vapour.

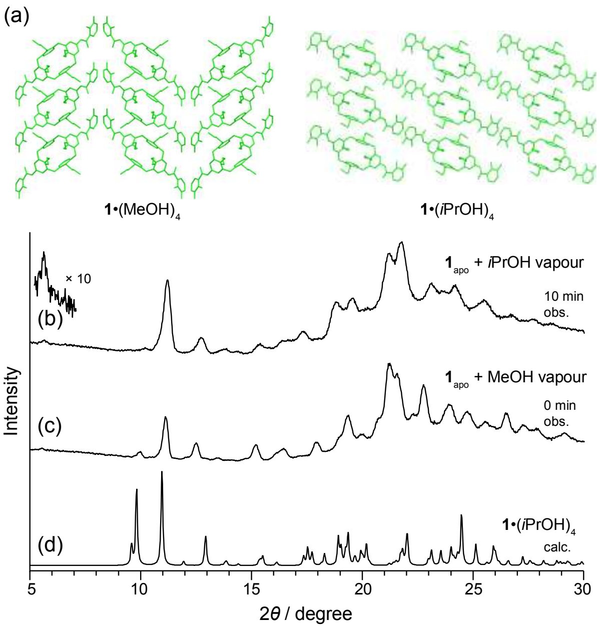

Fig. 9 (a) The crystal packing of (left) **1**•$(MeOH)_4$ and (right) **1**•$(i\text{PrOH})_4$. Only **1** is shown. Observed and calculated X-ray powder diffraction patterns (5° ≤ $2\theta \leq$ 30°) of (b) $\mathbf{1}_{apo}$+*i*PrOH, (c) $\mathbf{1}_{apo}$+MeOH, and (d) **1**•$(i\text{PrOH})_4$. Scan rate = 20 degree min^{-1}.

Conclusions

In conclusion, 5,17-difunctionalized calix[4]arene **1** is an excellent host for small organic molecules. The excellent molecular recognition properties of **1** originate from the induced-fit adjustments of the relative location of the columnar structures for the organic guests and the presence of hydrogen bond donor and acceptor sites on the catechol side arms. Head-to-tail columnar structures were found in all of the cocrystals except for **1**•$(H_2O)_2$, which formed a zigzag array of **1** instead. This difference demonstrates that the organic guests induced the formation of the crystal packing consisting of the head-to-tail columnar structures. The structure of the columnar assemblies was not distorted by hydrogen bonding, though only weak van der Waals interactions operate between the terminal methyl groups and the cavity of the calix[4]arene. The strong tendency toward head-to-tail columnar assembly is attributed to the structure of **1**; this structure includes hydrophilic catechol side arms and a hydrophobic calix[4]arene moiety. The organic guests selectively interact with the catechol side arms, while the calix[4]arene moieties form the columnar structure without interference by the organic guests. The adsorption experiments suggest that crystalline apohost $\mathbf{1}_{apo}$ has columnar structures similar to those found in **1**•$(MeOH)_4$, enabling the reconstruction of the original crystal packing after the adsorption of MeOH vapour.

Acknowledgements

We thank Prof. T. Ichikawa and Dr. T. Kimura for collecting the X-ray powder diffraction data. This work was supported by Grant-in-Aids for Scientific Research (B) (No. 21350066) and Challenging Exploratory Research (No. 21355105) of JSPS as well as by Grant-in-Aids for Scientific Research on Innovative Areas, “Stimuli-responsive Chemical Species for the Creation of Functional Molecules” and “New Polymeric Materials Based on Element-Blocks” (No. 25109529, 25102532).

Notes and references

Department of Chemistry, Graduate School of Science, Hiroshima University 1-3-1 Kagamiyama, Higashi-Hiroshima, 739-8526 Japan.

E-mail: haino@hiroshima-u.ac.jp

† Electronic supplementary information (ESI) available: crystallographic information files (CIFs) of **1**•(*n*PrOH)$_4$, **1**•(AcOH)$_4$, **1**•(AcOEt), **1**•(CH$_3$CN)$_2$, and **1**•(H$_2$O)$_2$. CCDC 987474-987478. For ESI and crystallographic data in CIF or other electronic format, see DOI: 10.1039/b000000x/

1. (a) V. Böhmer, *Angew. Chem. Int. Ed. Engl.*, 1995, **34**, 713-745; (b) A. Ikeda and S. Shinkai, *Chem. Rev.*, 1997, **97**, 1713-1734; (c) T. Schrader and A. D. Hamilton, *Functional Synthetic Receptors*, Wiley-VCH Verlag Gmbh & Co. KGaA. Weinheim, 2005; (d) C. D. Gutsche, *Calixarene: An Introduction, 2nd edn*, Royal Society of Chemistry, Cambridge, UK, 2008; (e) F. Perret and A. W. Coleman, *Chem. Commun.*, 2011, **47**, 7303-7319.
2. (a) M. A. McKervey, E. M. Seward, G. Ferguson and B. L. Ruhl, *J. Org. Chem.*, 1986, **51**, 3581-3584; (b) A. Ikeda and S. Shinkai, *J. Am. Chem. Soc.*, 1994, **116**, 3102-3110; (c) W. Verboom, O. Struck, D. N. Reinhoudt, J. P. M. van Duynhoven, G. J. van Hummel, S. Harkema, K. A. Udachin and J. A. Ripmeester, *Gazz. Chim. Ital.*, 1997, **127**, 727-739; (d) A. Faldt, F. C. Krebs and M. Jørgensen, *Tetrahedron Lett.*, 2000, **41**, 1241-1244; (e) M. O. Vysotsky, M. Bolte, I. Thondorf and V. Böhmer, *Chem. Eur. J.*, 2003, **9**, 3375-3382; (f) J. Sýkora, J. Budka, P. Lhoták, I. Stibor and I. Císařová, *Org. Biomol. Chem.*, 2005, **3**, 2572-2578; (g) T. E. Clark, M. Makha, C. L. Raston and A. N. Sobolev, *Cryst. Growth Des.*, 2006, **6**, 2783-2787; (h) G. Ramon, A. W. Coleman and L. R. Nassimbeni, *Cryst. Growth Des.*, 2006, **6**, 132-136; (i) T. E. Clark, M. Makha, A. N. Sobolev, S. J. Dalgarno, J. L. Atwood and C. L. Raston, *Cryst. Growth Des.*, 2007, **7**, 2059-2065; (j) J. Klimentová, P. Vojtíšek and M. Sklenářová, *J. Mol. Struct.*, 2007, **871**, 33-41; (k) F. Maharaj, D. C. Craig, M. L. Scudder, R. Bishop and N. Kumar, *J. Incl. Phenom. Macro.*, 2007, **59**, 17-24; (l) M. Mastalerz, H. J. E. Rivera, I. M. Oppel and G. Dyker, *CrystEngComm*, 2011, **13**, 3979-3982; (m) S. Kennedy, I. E. Dodgson, C. M. Beavers, S. J. Teat and S. J. Dalgarno, *Cryst. Growth Des.*, 2012, **12**, 688-697.
3. (a) G. D. Andreetti, R. Ungaro and A. Pochini, *J. Chem. Soc., Chem. Commun.*, 1979, 1005-1007; (b) R. Ungaro, A. Pochini, G. D. Andreetti and P. Domiano, *J. Chem. Soc., Perkin Trans. 2*, 1985, 197-201; (c) G. Calestani, F. Ugozzoli, A. Arduini, E. Ghidini and R. Ungaro, *J. Chem. Soc., Chem. Commun.*, 1987, 344-346; (d) E. B. Brouwer, J. A. Ripmeester and G. D. Enright, *J. Inclus. Phenom. Mol.*, 1996, **24**, 1-17; (e) E. B. Brouwer, K. A. Udachin, G. D. Enright and J. A. Ripmeester, *Chem. Commun.*, 2000, 1905-1906; (f) E. B. Brouwer, K. A. Udachin, G. D. Enright, J. A. Ripmeester, K. J. Ooms and P. A. Halchuk, *Chem. Commun.*, 2001, 565-566; (g) K. A. Udachin, G. D. Enright, E. B. Brouwer and J. A. Ripmeester, *J. Supra. Chem.*, 2001, **1**, 97-100; (h) J. A. Ripmeester, G. D. Enright, C. I. Ratcliffe, K. A. Udachin and I. L. Moudrakovski, *Chem. Commun.*, 2006, 4986-4996; (i) T. Gruber, M. Peukert, D. Schindler, W. Seichter, E. Weber and P. Bombicz, *J. Incl. Phenom. Macro.*, 2008, **62**, 311-324.
4. (a) J. L. Atwood, R. K. Juneja, P. C. Junk and K. D. Robinson, *J. Chem. Crystallogr.*, 1994, **24**, 573-576; (b) F. Arnaud-Neu, S. Fuangswasdi, A. Notti, S. Pappalardo and M. F. Parisi, *Angew. Chem. Int. Ed.*, 1998, **37**, 112-114; (c) D. Garozzo, G. Gattuso, F. H. Kohnke, P. Malvagna, A. Notti, S. Occhipinti, S. Pappalardo, M. F. Parisi and I. Pisagatti, *Tetrahedron Lett.*, 2002, **43**, 7663-7667; (d) D. Garozzo, G. Gattuso, F. H. Kohnke, A. Notti, S. Pappalardo, M. F. Parisi, I. Pisagatti, A. J. P. White and D. J. Williams, *Org. Lett.*, 2003, **5**, 4025-4028.
5. (a) A. W. Coleman, S. G. Bott, S. D. Morley, C. M. Means, K. D. Robinson, H. Zhang and J. L. Atwood, *Angew. Chem. Int. Ed. Engl.*, 1988, **27**, 1361-1362; (b) J. L. Atwood, G. W. Orr, F. Hamada, R. L. Vincent, S. G. Bott and K. D. Robinson, *J. Am. Chem. Soc.*, 1991, **113**, 2760-2761; (c) J. L. Atwood, G. W. Orr, N. C. Means, F. Hamada, H. Zhang, S. G. Bott and K. D. Robinson, *Inorg. Chem.*, 1992, **31**, 603-606; (d) N. Douteau-Guével, A. W. Coleman, J.-P. Morel and N. Morel-Desrosiers, *J. Phys. Org. Chem.*, 1998, **11**, 693-696; (e) N. Douteau-Guével, A. W. Coleman, J.-P. Morel and N. Morel-Desrosiers, *J. Chem. Soc., Perkin Trans. 2*, 1999, 629-633; (f) M. Selkti, A. W. Coleman, I. Nicolis, N. Douteau-Guével, F. Villain, A. Tomas and C. de Rango, *Chem. Commun.*, 2000, 161-162; (g) J. L. Atwood, L. J. Barbour, M. J. Hardie, C. L. Raston, M. N. Statton and H. R. Webb, *CrystEngComm*, 2001, **4**, 1-3; (h) J. L. Atwood, L. J. Barbour, S. Dalgarno, C. L. Raston and H. R. Webb, *J. Chem. Soc., Dalton Trans.*, 2002, 4351-4356; (i) J. L. Atwood, T. Ness, P. J. Nichols and C. L. Raston, *Cryst. Growth Des.*, 2002, **2**, 171-176; (j) G. Arena, A. Casnati, A. Contino, A. Magrì, F. Sansone, D. Sciotto and R. Ungaro, *Org. Biomol. Chem.*, 2006, **4**, 243-249; (k) S. J. Dalgarno, J. L. Atwood and C. L. Raston, *Cryst. Growth Des.*, 2006, **6**, 174-180; (l) W. Xiao, C. Hu and M. D. Ward, *Cryst. Growth Des.*, 2013, **13**, 3197-3200.
6. (a) T. Haino, T. Harano, K. Matsumura and Y. Fukazawa, *Tetrahedron Lett.*, 1995, **36**, 5793-5796; (b) T. Haino, K. Yamada and Y. Fukuzawa, *Synlett*, 1997, 673-674; (c) T. Haino, M. Yanase and Y. Fukazawa, *Angew. Chem. Int. Ed. Engl.*, 1997, **36**, 259-260; (d) T. Haino, H. Akii and Y. Fukazawa, *Synlett*, 1998, 1016-1018; (e) T. Haino, Y. Katsutani, H. Akii and Y. Fukazawa, *Tetrahedron Lett.*, 1998, **39**, 8133-8136; (f) T. Haino, K. Matsumura, T. Harano, K. Yamada, Y. Saijyo and Y. Fukazawa, *Tetrahedron*, 1998, **54**, 12185-12196; (g) T. Haino, M. Yanase and Y. Fukazawa, *Angew. Chem. Int. Ed.*, 1998, **37**, 997-998; (h) T. Haino, H. Araki, Y. Yamanaka and Y. Fukazawa, *Tetrahedron Lett.*, 2001, **42**, 3203-3206; (i) T. Haino, H. Araki, Y. Fujiwara, Y. Tanimoto and Y. Fukazawa, *Chem. Commun.*, 2002, 2148-2149; (j) T. Haino, Y. Yamanaka, H. Araki and Y. Fukazawa, *Chem. Commun.*, 2002, 402-403; (k) T. Haino, M. Nakamura, N. Kato, M. Hiraoka and Y. Fukazawa, *Tetrahedron Lett.*, 2004, **45**, 2281-2284; (l) T. Haino, Y. Matsumoto and Y. Fukazawa, *J. Am. Chem. Soc.*, 2005, **127**, 8936-8937; (m) T. Haino, C. Fukunaga and Y. Fukazawa, *Org. Lett.*, 2006, **8**, 3545-3548; (n) T. Haino, M. Nakamura and Y. Fukazawa, *Heterocycles*, 2006, **68**, 2477-2482; (o) T. Haino, M. Yanase, C. Fukunaga and Y. Fukazawa, *Tetrahedron*, 2006, **62**, 2025-2035; (p) T. Haino, H. Fukuoka, M. Katayama and Y. Fukazawa, *Chem. Lett.*, 2007, **36**, 1054-1055; (q) T. Haino, H. Fukuoka, H. Iwamoto and Y. Fukazawa, *Supramol. Chem.*, 2008, **20**, 51-57; (r) T. Haino, M. Hirakata, K. Niimi, M. Kouchi, H. Iwamoto and Y. Fukazawa, *Chem. Lett.*, 2008, **37**, 394-395; (s) T. Haino, H. Shio, R. Takano and Y. Fukazawa, *Chem. Commun.*, 2009, 2481-2483; (t) T. Haino, E. Hirai, Y. Fujiwara and K. Kashihara, *Angew. Chem. Int. Ed.*, 2010, **49**, 7899-7903.
7. R. Sekiya, Y. Yamasaki, S. Katayama, H. Shio and T. Haino, *CrystEngComm*, 2013, **15**, 8404-8407.
8. (a) T. Komori and S. Shinkai, *Chem. Lett.*, 1993, 1455-1458; (b) B. Xu and T. M. Swager, *J. Am. Chem. Soc.*, 1993, **115**, 1159-1160.
9. (a) M. Makha and C. L. Raston, *Chem. Commun.*, 2001, 2470-2471; (b) S. Cecillon, A. Lazar, O. Danylyuk, K. Suwinska, B. Rather, M. J. Zaworotko and A. W. Coleman, *Chem. Commun.*, 2005, 2442-2444.
10. G. M. Sheldrick, *Acta Crystallogr. Sect. A*, 2008, **64**, 112-122.
11. A. L. Spek, *Acta Crystallogr. Sect. D*, 2009, **65**, 148-155.
12. (a) M. A. Spackman and J. J. McKinnon, *CrystEngComm*, 2002, **4**, 378-392; (b) J. J. McKinnon, D. Jayatilaka and M. A. Spackman, *Chem. Commun.*, 2007, 3814-3816; (c) M. A. Spackman and D. Jayatilaka, *CrystEngComm*, 2009, **11**, 19-32.
13. J. Bernstein, R. E. Davis, L. Shimoni and N.-L. Chang, *Angew. Chem. Int. Ed.*, 1995, **34**, 1555-1573.
14. (a) G. R. Desiraju, *Angew. Chem. Int. Ed. Engl.*, 1995, **34**, 2311-2327; (b) G. R. Desiraju, *Chem. Commun.*, 1997, 1475-1482.
15. (a) P. Holý, J. Závada, I. Císařová and J. Podlaha, *Angew. Chem. Int. Ed.*, 1999, **38**, 381-383; (b) C. B. Aakeröy, A. M. Beatty and B. A. Helfrich, *J. Am. Chem. Soc.*, 2002, **124**, 14425-14432; (c) D. Das, R. K. R. Jetti, R. Boese and G. R. Desiraju, *Cryst. Growth Des.*, 2003, **3**, 675-681; (d) M. Gdaniec, W. Jankowski, M. J. Milewska and T. Połoñski, *Angew. Chem. Int. Ed.*, 2003, **42**, 3903-3906; (e) S. Kohmoto, Y. Kuroda, K. Kishikawa, H. Masu and I. Azumaya, *Cryst. Growth Des.*, 2009, **9**, 5017-5020.

16. (a) C. B. Aakeröy, A. M. Beatty and D. S. Leinen, *Angew. Chem. Int. Ed.*, 1999, **38**, 1815-1819; (b) R. Sekiya and S. Nishikiori, *Chem. Commun.*, 2001, 2612-2613; (c) G. Yang, H.-G. Zhu, B.-H. Liang and X.-M. Chen, *J. Chem. Soc., Dalton Trans.*, 2001, 580-585; (d) Z. Qin, M. C. Jennings, R. J. Puddephatt and K. W. Muir, *Inorg. Chem.*, 2002, **41**, 5174-5186; (e) R. Sekiya and S. Nishikiori, *Chem. Eur. J.*, 2002, **8**, 4803-4810; (f) R. Sekiya, S. Nishikiori and K. Ogura, *J. Am. Chem. Soc.*, 2004, **126**, 16587-16600.

TOC graphic

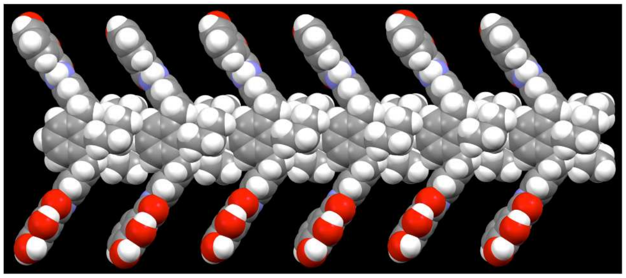

Calix[4]arenes often form dimeric capsules or up-down bilayer arrangements in the solid state. The head-to-tail polymeric columnar structure found in the cocrystals composed of 5,17-difunctionalized calix[4]arene **1** and organic guests represents another structural motif for calix[4]arenes.